Journal of Magnetics 4(1), 26-32 (1999)

Thermomagnetic Characteristics of the Hard Magnetic Materials with a Fine Microstructure due to a HDDR Process

H. W. Kwon, Yoon B. Kim* and W. Y. Jeung*

Pukyong National University, Pusan, South Korea
**Metal Processing Research Centre, Korea Institute of Science and Technology, Seoul, South Korea*

(Received 1 February 1998)

The HDDR process can be used as an effective means of processing of the coercive Nd-Fe-B-type or the $Sm_2Fe_{17}N_x$ materials. The HDDR (hydrogenation, disproportionation, desorption, recombination) processed materials are featured with a very fine microstructure. The thermomagnetic characteristics of the Nd-Fe-B-type or the $Sm_2Fe_{17}N_x$ materials with fine microstructure due to the HDDR process were investigated. It has been found that the fine-microstructured hard magnetic materials showed an unusual TMA (Thermomagnetic analysis) tracing featured with a low and constant magnetization at lower temperature range and a peak just below their Curie temperatures when a low external field is applied. This unusual thermomagnetic characteristic was immediate particularly in the TMA with a low applied field. This thermomagnetic characteristic was interpreted in terms of the competition between two counteracting effects; the decrease in magnetization due to the thermal agitation at an elevated temperature and the increase in magnetization resulting from the rotation of magnetization of the fine grains comparable to a critical single domain size due to the decreased magnetocrystalline anisotropy at an elevated temperature.

1. Introduction

Since the discovery of Nd-Fe-B-type alloy in 1983 an extensive research effort has been made to develop new fabrication processes of the material into a useful permanent magnet. Among the variety of fabrication processes, the HDDR (hydrogenation, disproportionation, desorption, and recombination) process [1, 2] is considered to be a unique process in that the magnetically non-coercive Nd-Fe-B-type cast ingot material can be transformed easily to a magnetically coercive material simply by reacting the ingot material with hydrogen gas. The HDDR process is, thus, believed to be an effective means of producing the Nd-Fe-B-type powder with high coercivity. Meanwhile, there has been an extensive research effort to search for new potentially useful hard magnetic materials in addition to the Nd-Fe-B-type material. This search effort has brought to light a number of interesting new intermetallic compounds including $R_3(Fe,M)_{29}$-type compound [3-5] and $Sm_2Fe_{17}N_x$ [6-9] or $Sm_2Fe_{17}C_x$ [10, 11]. Among the new potential materials, the $Sm_2Fe_{17}N_x$ material has been accepted to be a promising candidate for a useful permanent magnetic material. This material is usually prepared by the solid-gas reaction between finely milled Sm_2Fe_{17} alloy and nitrogen gas. It has been found that the HDDR process can also be used as an effective pre-treatment for an easy preparation of the nitride material [8, 12]. The HDDR process can, therefore, be used as an effective means of processing the coercive Nd-Fe-B-type and the $Sm_2Fe_{17}N_x$ materials. It is obvious that the HDDR processed materials may be featured with a very fine microstructure. The Nd-Fe-B-type or $Sm_2Fe_{17}N_x$ materials with fine microstructure due to the HDDR process are supposed to show a distinct magnetic characteristics with respect to the materials with coarse grain structure. The principal purpose of the present study is to investigate the thermomagnetic characteristics of the Nd-Fe-B-type or the $Sm_2Fe_{17}N_x$ material processed with by HDDR and to compare them with those of the materials with coarse grain structure and fine-grained melt-spun material.

2. Experimental Works

Nd-Fe-B-type alloy and Sm_2Fe_{17} parent alloy for the $Sm_2Fe_{17}N_x$ material were produced by an induction melting of the high purity constituting elements under Ar gas atmo-

Table 1. Chemical compositions of the materials used

Material	Content (at%)				
	Nd	Sm	Fe	Co	B
Nd-Fe-B-type	16.0		76.0		8.0
Sm_2Fe_{17}-type		10.1	89.9		
MQP-D	12.3		65.1	16.6	6.0

Table 2. HDDR, nitrogenation conditions used

		Nd-Fe-B-type	$Sm_2Fe_{17}N_x$	
			HDDR + nitrogenation	conventional
HDDR	Hydrogenation	heating up to 800°C under hydrogen gas (H_2 pressure : 1.2 bar)	heating up to 750°C under hydrogen gas (H_2 pressure : 1.4 bar)	
	Disproportionation	holding at 800°C for 2 hrs under hydrogen gas (H_2 pressure: 1.2 bar)	holding at 750°C for 2 hrs under hydrogen gas (H_2 pressure : 1.4 bar)	
	Desorption and recombination	holding at 800°C for 1 hr under vacuum	holding at 750°C for 2 hrs under vacuum	
Nitrogenation			at 450°C for 12 hrs (N_2 pressure : 1.8 bar)	at 475°C for 17 hrs (N_2 pressure: 1.8 bar)

sphere. Composition of the alloys used in the present study is tabulated in Table 1. The prepared Nd-Fe-B-type alloy ingot was homogenized at 1000 °C for 5 hrs, and the Sm_2Fe_{17}-type alloy at 1000 °C for 2 weeks under Ar gas atmosphere. The homogenized Nd-Fe-B-type alloy was crushed into a coarse particle (around 3 mm) and then subjected to a standard HDDR treatment (see Table 2). The homogenized Sm_2Fe_{17} alloy was first crushed into a powder with particle size of around 60 μm and then subjected to a HDDR process prior to nitrogenation. The HDDR-treated Sm_2Fe_{17} material was nitrogenated at 450 °C for 12 hrs. The $Sm_2Fe_{17}N_x$ material was also prepared by a conventional way consisting of nitrogenation only. The homogenized alloy was crushed into powders with finer particle size of around 20 μm and then nitrogenated at 475 °C for 12 hrs. The HDDR and/or nitrogenation conditions used for the preparation of the $Sm_2Fe_{17}N_x$ materials are also tabulated in Table 2. Magnetic characterization of the materials was performed using a VSM after pulsing magnetization with field of 4.5 T. Thermomagnetic characteristics of the materials were examined using a Sucksmith-type balance [13] with varying applied field. In addition to the fine microstructured Nd-Fe-B-type or $Sm_2Fe_{17}N_x$ materials due to the HDDR, the melt-spun ribbon (MQP-D) with fine microstructure and the homogenized Nd-Fe-B-type alloy were also used for comparison. The MQP-D material was supplied by Magnequench, and its chemical composition was also included in Table 1.

3. Results and Discussion

Prior to investigating the thermomagnetic characteristics of the HDDR treated Nd-Fe-B-type and the $Sm_2Fe_{17}N_x$ materials, the magnetic properties of the materials were examined. It has been found that the HDDR treated Nd-Fe-B-type shows a considerably high intrinsic coercivity (9.1 kOe). It was notable that the $Sm_2Fe_{17}N_x$ material produced by HDDR and nitrogenation has a high intrinsic coercivity (12.9 kOe) even in the state of coarse particle (60 μm) whereas the material produced by the conventional way exhibited very low intrinsic coercivity in the state of coarse particle (20 μm). The high coercivity of the HDDR processed Nd-Fe-B-type and the $Sm_2Fe_{17}N_x$ material produced by HDDR and nitrogenation even in the state of coarse particle may, needless to say, be attributed to the microstructure of particle consisting of very fine grains comparable to its critical single domain size (0.3 μm) due to the HDDR process. The low coercivity of the $Sm_2Fe_{17}N_x$ material produced by the conventional way may be attributed to the microstructure of particle consisting of probable single grain (20 μm) far greater than the critical single domain size. However, the coercivity of this material can probably be enhanced if the particle size is further reduced. The intrinsic coercivity of the material milled down to fine particle (around 3 μm) appeared to be as high (12.8 kOe) as the value of the material produced by the HDDR and nitrogenation. These high coercivities indicate that the Nd-Fe-B-type alloy may have been optimally HDDR treated and the Sm_2Fe_{17} alloys may have been fully nitrogenated. It is, therefore, understood that the materials processed with the HDDR in the present study may have very fine microstructure consisting of the grains comparable to the critical single domain size. These optimally HDDR treated Nd-Fe-B-type alloy and $Sm_2Fe_{17}N_x$ materials were used for examining their thermomagnetic characteristics.

In order to see the thermomagnetic characteristic of the HDDR treated Nd-Fe-B-type, Thermomagnetic analysis (TMA) was performed under a low applied field (0.8 kOe), and the result is shown in Fig. 1. Also shown in Fig. 1 is the TMA tracing for the homogenized Nd-Fe-B-type alloy for comparison. The low field TMA tracings were also performed for the $Sm_2Fe_{17}N_x$ materials produced by the HDDR and nitrogenation, and the result is shown in Fig. 2. Also shown in Fig. 2 is the TMA tracing for the $Sm_2Fe_{17}N_x$ material produced by the conventional way. It appears that the Nd-Fe-B-type material or $Sm_2Fe_{17}N_x$ material processed by HDDR shows a distinct thermomagnetic characteristic from the materials not HDDR processed. On heating the magnetization of the HDDR processed materials remains unexpectedly almost constant up to a certain temperature (around 160 °C for Nd-Fe-B-type, and around 375 °C for $Sm_2Fe_{17}N_x$), from which it begins to increase and shows a

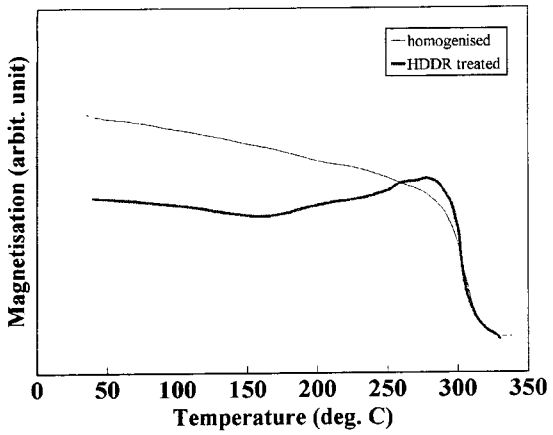

Fig. 1. TMA tracings of the HDDR treated or homogenized Nd-Fe-B-type alloy.

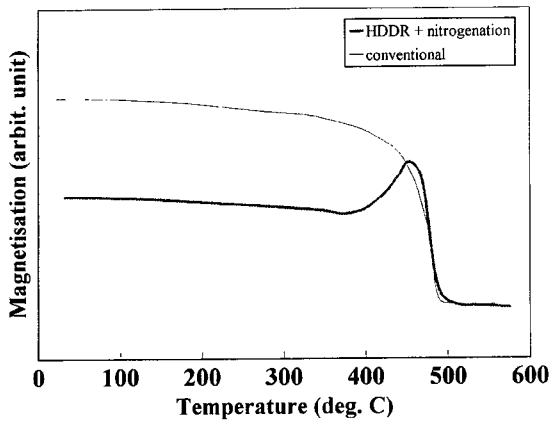

Fig. 2. TMA tracings of the $Sm_2Fe_{17}N_x$ materials prepared by the HDDR and nitrogenation or by the conventional way.

peak just below the Curie temperature.

Thermomagnetic properties of the HDDR processed materials were examined in more detail by performing the TMA tracings under various conditions. The materials were heated above their Curie temperatures and then cooled

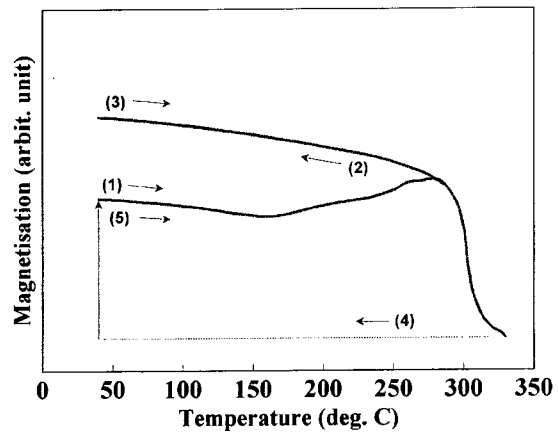

Fig. 3. TMA tracings performed under various conditions for the HDDR treated Nd-Fe-B-type alloy; (1) first heating, (2) cooling under an applied field, (3) second heating after cooling under an applied, (4) cooling without applied field, (5) second heating after cooling without an applied field.

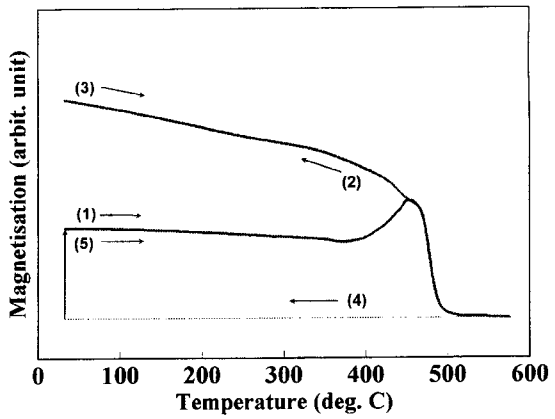

Fig. 4. TMA tracings performed under various conditions for the $Sm_2Fe_{17}N_x$ material produced by the HDDR and nitrogenation; (1) first heating, (2) cooling under an applied field, (3) second heating after cooling under an applied field, (4) cooling without an applied field, and (5) second heating after cooling without an applied field.

down to room temperature under the applied field. During this cooling TMAs were carried out and the results were given as (2) in Fig. 3 and Fig. 4. It can be seen that the TMA tracings on the cooling do not trace the change observed on heating. Instead a typical ferromagnetic behavior, in which a magnetization increases gradually with decreasing temperature, is observed. The materials cooled down to room temperature under the applied field were subjected again to heating TMA, and these second heating TMAs were given as (3) in Fig. 3 and Fig. 4. It appears that these results are almost identical to those observed on cooling under the applied field. It should be interesting, then, to examine the TMA tracing on the second heating for the materials cooled down without an applied field from above the Curie temperature after the first run, and the results of this run are given as (5) in Fig. 3 and Fig. 4. It is notable that the TMA tracings on the second heating after the cool-

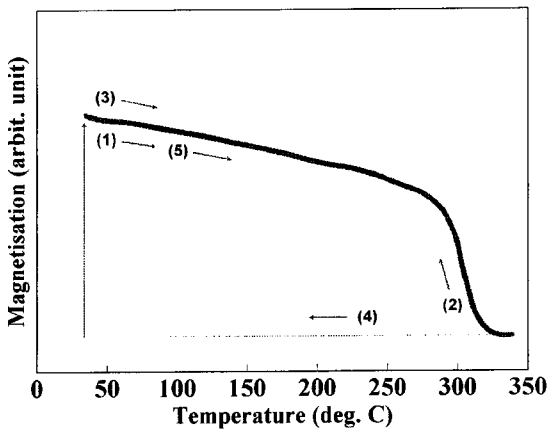

Fig. 5. TMA tracings performed under various conditions for the homogenized Nd-Fe-B-type alloy; (1) first heating, (2) cooling under an applied field, (3) second heating after cooling under an applied field, (4) cooling without an applied field, and (5) second heating after cooling without an applied field.

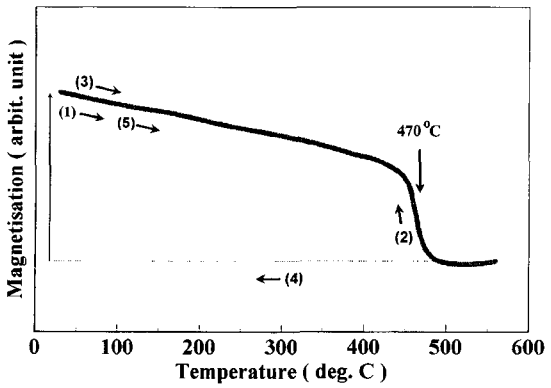

Fig. 6. TMA tracings performed under various conditions for the $Sm_2Fe_{17}N_x$ material produced by the conventional way; (1) first heating, (2) cooling under an applied field, (3) second heating after cooling under an applied field, (4) cooling without an applied field, and (5) second heating after cooling without an applied field.

ing without an applied field show an identical trend with those of the first heating. Meanwhile, the homogenized Nd-Fe-B-type and $Sm_2Fe_{17}N_x$ materials not HDDR processed were also subjected to the identical TMA tracings with those for the HDDR processed materials, and the results are shown in Fig. 5 and Fig. 6. It appears that, unlike the HDDR processed materials the materials, not HDDR processed show a typical ferromagnetic character regardless of the state of the sample during the TMAs.

We explain the above distinct TMA character of the HDDR processed materials in a manner proposed by the model shown in Fig. 7. In order to well understand the thermomagnetic characteristic of the HDDR processed materials, it is important to note the microstructural feature and magnetic domain structure of the materials. The HDDR treated Nd-Fe-B-type alloy and the $Sm_2Fe_{17}N_x$ material produced by the HDDR and nitrogenation may consist of very fine grains comparable to its critical single domain size (around 0.3 μm) due to the HDDR treatment [14]. The microstructure and domain structure of the HDDR processed materials is, therefore, expected to be like that proposed in Fig. 7, in which the magnetization of each grain

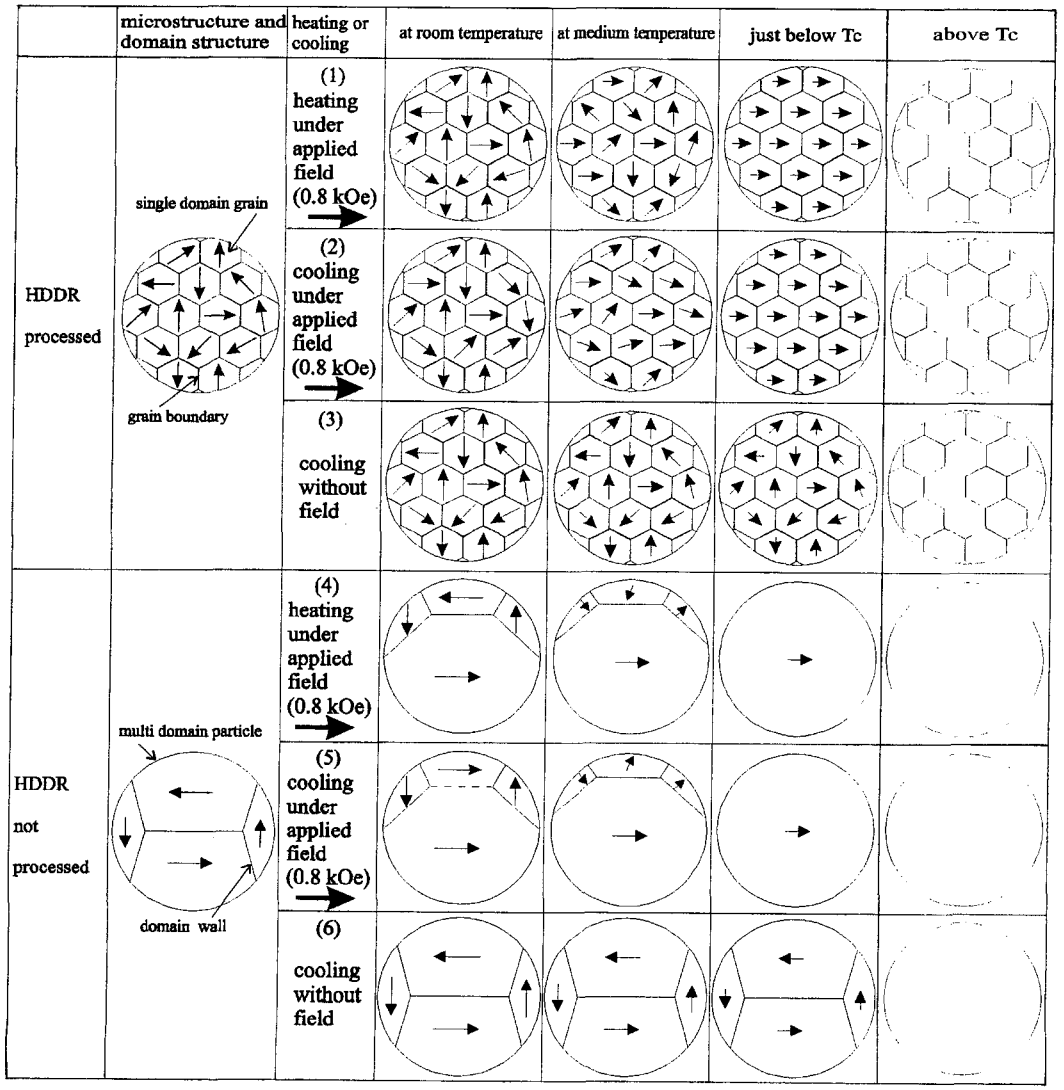

Fig. 7. Schematic diagram showing the change of magnetic domain structure of the materials during TMA.

points randomly. When these materials are placed under a weak applied field (0.8 kOe) at lower temperatures, little magnetization may be observed because there is no magnetic domain wall to move and the applied field is too weak to rotate the magnetization of grains along the applied field. $Nd_2Fe_{14}B$ and $Sm_2Fe_{17}N_x$ materials are known to have high magnetocrystalline anisotropy [15]. When these materials are heated up to a moderate temperature under the applied field two effects counteracting each other may take place. There will be a decrease in magnetization due to a thermal agitation of the magnetic moment. At the same time, as the temperature increases the magnetocrystalline anisotropy will be reduced, and this will give rise to an easy rotation of magnetization of the grains along the applied field, thus leading to an increase in magnetization. These two effects counteract each other, thus no significant magnetization change may be observed up to a moderate temperature. If the sample is heated further toward the Curie temperature the magnetization of each grain will be reduced further, and at the same time the magnetization rotation along the applied field may become much easier and a significant increase in magnetization may take place. The latter may be dominant in the competition at an elevated temperature, thus leading to an increase in magnetization. When the sample is heated close to the Curie temperature the decrease in magnetization due to the thermal fluctuation may become more dominant, and this may be responsible for the appearance of a peak just below the Curie temperature ((1) in Fig. 3 or Fig. 4).

The cooling TMA tracing under the applied field showed a different behavior from that of the heating, and this can be explained in the way proposed also in the model shown in Fig. 7. When the sample is heated above the Curie temperature the atomic magnetic moments of the material will be arranged in a paramagnetic mode. If the sample is cooled down, these randomly oriented moments will be aligned along the applied field on cooling through the Curie temperature. As the temperature decreases every magnetization of grains tends to turn back to its nearest easy magnetization direction. This means that magnetizations of all grains distribute more or less in favourable fashion with respect to the applied field. A great degree of alignment of each grain magnetization may, therefore, be maintained throughout the cooling. Under this circumstance, the increase in magnetization cooling due to the reduced thermal agitation may be dominant. This phenomenon may explain the typical gradual increase in magnetization on cooling under the applied field ((2) in Fig. 3 or Fig. 4). The TMA tracing for the sample previously heated above the Curie temperature and then cooled without the applied field showed an identical result with that of the first heating TMA. In this particular case, the atomic magnetic moments in each grain orient to grain easy magnetization direction on cooling through the Curie temperature, and the magnetic domain structure at room temperature may become random,

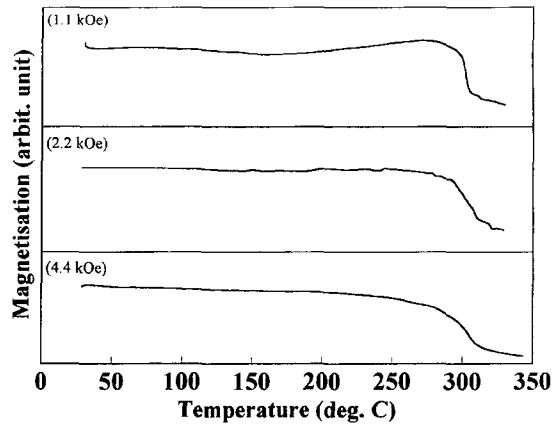

Fig. 8. TMA tracing of the HDDR treated Nd-Fe-B-type alloys with various applied field.

which may be the same as that before subjecting to the first run. Thus the TMA tracing for this sample should show an identical trend with that of the first run.

We explained the magnetization increase in TMA of the HDDR processed materials at an elevated temperature in terms of the competition between the thermal agitation and the magnetization rotation. If this interpretation is acceptable, the appearance of the magnetization bump should be influenced by the strength of the applied field of TMA run. As the strength of the applied field increases, the magnetization rotation may become easier, and the magnetization rotation would take place even at low temperature under a sufficiently high field. This fact suggests that the set-off temperature of the increase of magnetization due to the magnetization rotation in the TMA tracing would move toward lower temperature as the field strength increases. This argument was verified by the TMA tracings performed under various strengths of the applied field as shown in Fig. 8 and Fig. 9.

The thermomagnetic behaviour of the Nd-Fe-B-type or $Sm_2Fe_{17}N_x$ materials not HDDR processed may be explained in similar way using the model proposed in Fig. 7. In these materials each particle may probably consist of a

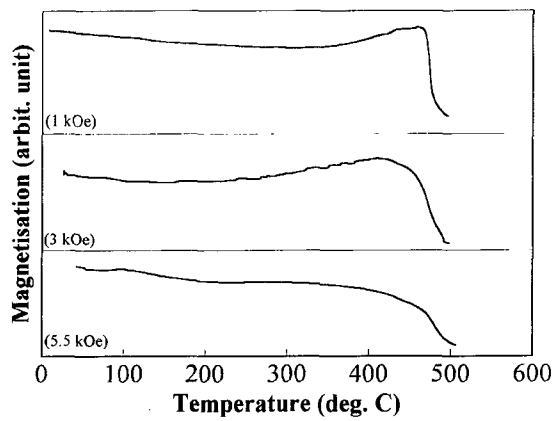

Fig. 9. TMA tracing of the $Sm_2Fe_{17}N_x$ material prepared by the HDDR and nitrogenation with various applied field.

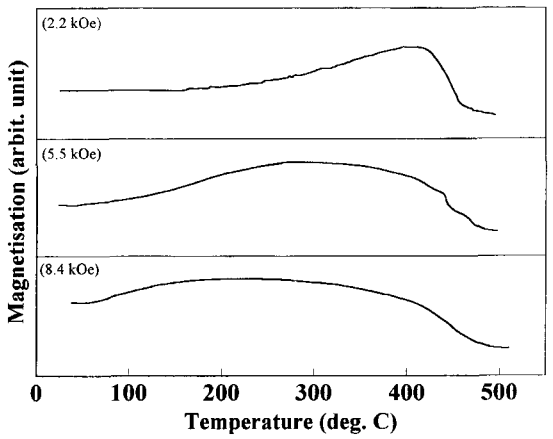

Fig. 10. TMA tracings of the MQP-D material with various applied field.

large single grain (around 20 μm) containing multiple magnetic domains, and its domain magnetizations may be isotropically distributed as shown in Fig. 7. When these materials are placed under the applied field (0.8 kOe) the domain wall may be moved easily and the favourably oriented domain may grow and predominate in the domains. This will result in a significant magnetization on applying magnetic field at room temperature. As the temperature increases the two counteracting effects discussed previously, of course, compete with each other. However, the increase in magnetization resulting from the rotation of magnetization in each domain due to the decrease in magnetocrystalline anisotropy at an elevated temperature may not be significant. The reason for this can be explained as follows. As soon as the magnetic field is applied at room temperature, the domain walls move and most of the region in the particle may be occupied by the favourably oriented domain. Magnetization of the grown domain may be almost parallel to the applied field as suggested in Fig. 7. Thus the contribution of magnetization rotation to the magnetization increase at an elevated temperature may be resulted mainly from the unfavourably oriented small domains. This contribution may be very small, thus the decrease in magnetization due to the thermal agitation at an elevated temperature may become dominant all the way. This may explain the typical TMA tracing of the first run as shown in Fig. 5 and Fig. 6. The identical TMA tracing on the second heating after the cooling from above the Curie temperature under the applied field can be explained in a similar way as discussed for the material produced by the HDDR and nitrogenation. The TMA tracing on the second heating after the cooling without the applied field also showed an identical trend as shown in Fig. 5 and Fig. 6. This can be explained easily by considering the fact that, on cooling from above the Curie temperature without the applied field, the magnetic domain structure returns to the initial pattern before subjecting to the first run because of the absence of constraining applied field.

We explained the distinctive thermomagnetic characteristic of the HDDR processed materials in terms of the competition between two counteracting effect. This explanation may be applied to any type of hard magnetic material with very fine microstructure. It should, therefore, be interesting to see the TMA tracing of Nd-Fe-B melt-spun ribbon (MQP-D) which has a very fine microstructure. The TMA tracings for the material with varying applied field are shown in Fig. 10. The magnetization increase just below the Curie temperature during the TMA with low applied field is clearly observed.

4. Conclusions

The thermomagnetic characteristic of the hard magnetic materials with fine microstructure was investigated using the HDDR treated Nd-Fe-B-type or $Sm_2Fe_{17}N_x$ materials prepared by the HDDR and nitrogenation. It has been found that the fine-microstructured hard magnetic materials showed an unusual TMA tracing featured with a low and constant magnetization at lower temperature range and a peak just below the Curie temperature. This unusual thermomagnetic characteristic was immediate particularly when the applied field was low. This thermomagnetic characteristic was interpreted in terms of the competition between two counteracting effects; the decrease in magnetization due to the thermal agitation at an elevated temperature and the increase in magnetization resulting from the rotation of magnetization in the fine grains comparable to a single domain size, due to the decreased magnetocrystalline anisotropy at an elevated temperature.

Acknowledgement

The authors would like to acknowledge gratefully that the present work was supported by the Academic Research Fund for Advanced Materials in 1997 of the Ministry of Education, Republic of Korea. Thanks are also due to the MOST for support of the G7 project of which this work forms a part.

References

[1] T. Takeshita and R. Nakayama, Proc. 10th Int. Workshop on RE Magnets and Their Applications, Kyoto, Japan, 551 (1989).
[2] I. R. Harris, Proc. 12th Int. Workshop on RE Magnets and Their Applications, Canberra, Australia, 347 (1992).
[3] J. M. Cadogan, H. S. Li, A. Margarian, J. B. Dunlop, D. H. Ryan, S. J. Collocott, and R. L. Davis, J. Appl. Phys., **76**, 6138 (1994).
[4] Z. Hu and W. B. Yelon, Solid State Commun., **91**, 223 (1994).
[5] D. Courtois, H. S. Li, J. M. Cadogan, D. Givord, and E. Bourgeat-Lami, IEEE Trans. Magn. MAG-33, 3844 (1997).
[6] J. M. D. Coey, H. Sun, J. Magn. Magn. Mat., **87**, L254 (1990).

[7] P. G. McCormick and D. Maurice, Proc. 13th Int. Workshop on RE Magnets and Their Applications, Birmingham, U.K., 781 (1994).
[8] P. A. P. Wendhausen, B. Gebel, N. M. Muller, J.M.D. Coey, Proc. 13th Int. Workshop on RE Magnets and Their Applications, Birmingham, U.K., 831 (1994).
[9] H. W. Kwon, Journal of Magnetics, **1**, 19 (1996).
[10] Z. H. Cheng, B. G. Shen, J. X. Zhang and F. W. Wang, J. Appl. Phys., **76**, 6734 (1994).
[11] Y. H. Zheng, A. S. Murthy, F. M. Yang, and G. C. Hadjipanayis, J. Magn. Magn. Mat., **1081**, 140 (1995).
[12] N. M. Dempsey, P. A. P. Wendhausen, B. Gebel, K. H. Muller and J.M.D. Coey, Proc. 14th Int. Workshop on RE Magnets and Their Applications, Sao Paulo, Brazil, 349 (1996).
[13] S. Chikazumi, *Physics of Magnetism*, John Wiley & Sons, 29 (1964).
[14] David Book and I. R. Harris, Proc. 8th Intl Symposium on Magnetic Anisotropy and Coercivity in RE-TM Alloys, (1996) 205.
[15] B. P. Hu and J. M. D. Coey, J. Less-Common Met., **71**, 33 (1991).